ATLANTIS PRESS

Advances in Engineering Research (AER), volume 105

3rd Annual International Conference on Mechanics and Mechanical Engineering (MME 2016)

Testing Research on the Deformation Mechanism of High Manganese Steel and the Model of Surface Roughness Machined at High-Speed Cutting

Hu-Ping AN [1, 2*], Zhi-Yuan RUI [2], Jun-Feng GUO [2]

[1]College of BaiLei Mechanical Engineering, Lan Zhou City University, Lanzhou 730070, China

[2]College of Mechano-Electronic Engineering, Lanzhou Univ. of Tech., Lanzhou 730050, China

1ahp2004@126.com, 2zhiy_rui@163.com, 2junf_guo@163.com

Keywords: High-speed cutting, High manganese steel, Ceramal tool, Deformation mechanism, Surface quality.

Abstract. To study the deformation mechanism of high manganese steel at high-speed machining and the influence of cutting parameters on a quality of machined surface and on a tool wear, we conducted a serial of tests cutting high manganese steel with metal ceramic tool. By observing the macroscopic chip and measuring its micro-morphology with optical microscope under the condition of five groups of cutting parameters, the effect of cutting speed and amount of feed on chip shape was analyzed. The main mechanism of chip deformation and its effect on chip morphology and tool wear has been studied, and a linear model of surface roughness has been built with regression test method for predicting machined quality. The results show that the deformation mechanism of high manganese steel at high-speed cutting is the concentrated shear or adiabatic shear, and the reason of tool wear is a coherent wear combining abrasive wear and oxidative wear. The model of surface roughness obtained can preferably be used to forecast the machined surface quality by given cutting parameters, or determine cutting parameters with the required roughness height.

High manganese steel is the typical wear-resistant steel with advantages of good castability and low cost. Under the condition of a strong load, the surface of high manganese steel part is intensified due to work hardening, and its surface texture becomes martensite from austenite, and hardness increase to 450~550HB from 180~220HB while its keeps the original property in nexine. Therefore, high manganese steel has been widely used because of its high abrasive resistance, shock resistance and antifatigue crack. However, no other than the surface hardening, low heat conductivity coefficient, large elongation and deformation coefficient, it presents high cutting temperature, big cutting force, serious wear of tool and formed built-up edge when high manganese steel is being machined, which is then hard to control the machining precision and surface quality and to break up the chip. Hence, high manganese steel belongs to difficult-to-process material. The cost to process it is high and the range of application is limited. Hu yong-ke [1] makes a research on the processing technic of high manganese steel, summarizing the method of choosing tool material and geometrical parameters. Xu li et al. [2] set up a constitutive model of the plastic deformational behavior of high manganese steel, which can provide a basis for emulate study the cutting property. Xu yu-dong et al. [3-4] studied the matching of metal ceramic tool to process the high manganese steel, which indicates that the tool is not suit for cutting chilled cast iron. Liu zhan-qiang, Ai Xing et al[5-6]. studied the synthesis technique of high-speed cutting (HSC) and abrasion morphology of tool surface, which proved the advantages of high speed cutting. In consideration of the character of high manganese steel and the advantage of HSC, the cutting deformation morphology was observed and analyzed by an experiment of HSC with metal ceramic tool to cut high manganese steel in this paper so as to research the behavior of chip transformation and tool wear mechanism. The model of surface roughness with cutting parameters is obtained, which can offer a basis for choosing process parameters before HSC.

Experimental Condition

Workpiece Material

The material used in test is high manganese steel (ZGMn13), and the metallographic structure of it is austenite and carbide. The main mechanics performances contain strength of extension σ_b=980MPa, and hardness180~220HBW, and limit of yielding strength $\sigma_s \geq$295MPa, and ductility δ=50%~80%, and impact toughness $\alpha_k \geq 149 J/cm^2$, and heat conductivity coefficient k=13W/(m·K). High manganese steel tube used in the test is of a length of 330 mm, and an outer diameter of 168 mm, and a wall thickness of 20 mm. The chemical component of the steel is shown in table 1.

Table 1. Chemical components of high manganese steel

Elements	Mn	C	Si	P	S
Mass fraction	11~14	1.0~1.4	0.3~1.0	<0.03	<0.05

Cutter Material and Its Geometrical Parameters

Metal ceramic is a composite material of ceramic and metal, taking metal carbide as a hard phase occupy more than 80% and the others as binding phase of metallic elements. Addition of metallic element makes the physical and mechanical properties of metal ceramic improve, and its hardness and heat resistance is higher than cemented carbide closing to ceramic while the flexure strength and fracture toughness property of it is higher than ceramic. Then, the metallic ceramic has a good combination property. Under the conventional cutting speed, the cermet tool has a better property than carbide tool while it is awaited an experimental research under the condition of high speed and dry cutting. The composition of the tool material used in this experiment is TiCN-Al_2O_3-Ni-Mo, marked with RCHT01 and SNMN150708 T03030. The mechanical property of this material is bending strength of σ_b=700~1000MPa, and hardness of HRA93-95. The geometrical parameters of the blade include size 15.875×15.875×7.94 and geometric angle showed in table 2.

Table 2. Geometrical parameters of tool

Geometrical Parameters	rake angle γ_o/(°)	rear angle α_o/(°)	edge angle λ_s/(°)	corner radius r_ε/(mm)	chamfer $b_{o1}\times\gamma_{o1}$/(mm×°)
value	0	0	0	1.6	0.3×30

Testing Program

This test is performed on a digital controlled lathe marked CAK6150D. The cutting speed(v_c) is changed by altering the revolution speed of the main shaft and a little change of workpiece diameter. At the same time, an amount of feed is adjusted by changing the feed speed(v_f) and the revolution speed(n)of the main spindle. The measurement of chip microscopic state is on an optical electron microscope (SEM). The abrasion loss of flank surface of cutting tool is measured on a tool microscope. The roughness of finished surface is surveyed by a digital roughness meter. A two-factor method is applied to study the effect of cutting speed and amount of feed on a chip deformation and a quality of finished surface and the tool wear. The test in a dry cutting is carried out with five-group different cutting speed and amount of feed and a constant depth of cut, which is showed in table 3.

Table 3. Cutting parameters in the test

Test number	1	2	3	4	5
Cutting speed v_c/(m/min)	245.31	386.22	474.925	560.49	688.84
Amount of feed f/(mm/r)	0.2	0.125	0.1	0.083	0.067
Depth of cut a_p/(mm)	0.25	0.25	0.25	0.25	0.25

Experimental Results and Analysis

Chip Form and Its Deformation Mechanism

The cutting tests are carried on according to table 3. The samplings of chip are measured and its morphology obtained is as follow.

(1)When the cutting parameters are cutting speed of v_c=245.31m/min, and amount of feed of f=0.2mm/r, and depth of cut of a_p=0.25mm, the macroscopic chip is showed in Fig.1 (a). The chip appearance is a continuous C-shape. It indicates that the chip has a nonuniform local deformation but not enough to fracture. The reason of it is due to the bigger amount of feed increasing the thickness of chip, while a deformation hardening makes the chip crisp but not enough to crack. The micromorphology of the chip underside and the top face are shown in Fig.1 (b) and (c), respectively. The underside form presents a local burn feature, it shows the heat of deformation and friction that caused the temperature on the chip underside exceeding the melting points of some chemical elements and then make them melt, such as element C, S, P. As different element has different melting point, a low melting point element forms a bigger molten bath, otherwise, appearing lesser one. Hence, three spots vary in size. The concave-convex serration can be seen on top surface of chip in the microscopic picture, which shows that serration chip arises under the condition of high-speed cutting. Seeing from the top face of chip, only light and shade peak valley can be seen. If it were observed from side-on of chip sample, the serration shape would be very evident. Due to high toughness of high manganese steel, serration top surface presents a larger plastic deformation feature.

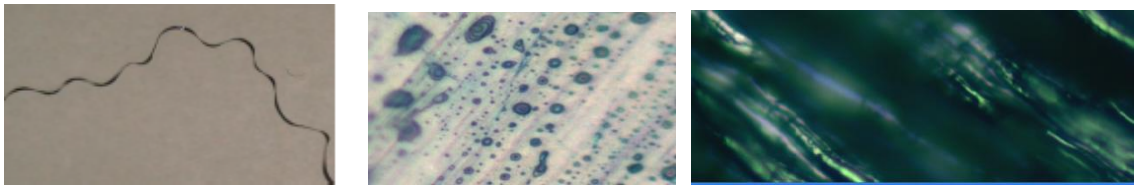

(a)Macroscopic shape (b)Undersurface (50X) (c)Top face (50X)

Figure.1. Chip shape (v_c=245.31 mm/min, f=0.2mm/r, a_p=0.25mm)

(2)When the cutting parameters are cutting speed of v_c=386.22m/min, amount of feed of f=0.125mm/r, depth of cut a_p=0.25mm, the macroscopic shape of the chip is showed in Fig. 2 (a). It can be seen that the chip basically appears a long band until an intertangling at the end is found, which go against the cutting process. The reason of it is the decrease of amount of feed that makes the chip thin and toughen, and then cutting temperature rises. The microscopic photo of chip underside and top face are showed in Fig.2 (b) and (c). It can be known that a continuous burn color and melting trace from the underside photo, which indicates that the cutting temperature is high. The reason of it is a smaller thickness of chip and its lower heat capacity make the temperature rise. It can be seen that the serration appears from the top face of chip with amaranth, which showed a higher cutting temperature.

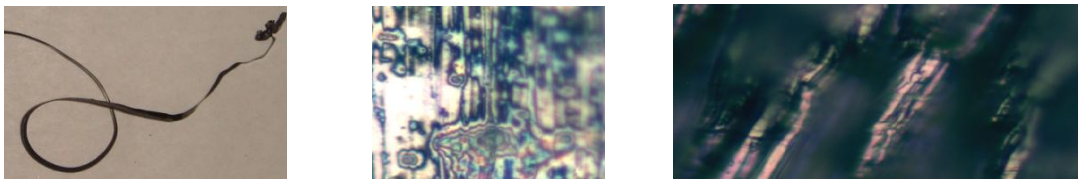

(a)Macroscopic shape (b)Undersurface(50X) (c)Top face(50X)

Figure.2. Chip shape (v_c=386.22m/min, f=0.125mm/r, a_p=0.25mm)

(3)As cutting parameters are v_c=474.925m/min, f=0.1mm/r, and a_p=0.25mm, respectively, the macroscopic shape of chip is showed in Fig.3 (a). It shows that the chip shape changes obviously and presents successive C-shape, which makes for cutting process and break up chip. The

microstate of the underside and top face of chip is showed in Fig.3 (b) and (c). It can be seen that the burn degree of chip and the cutting temperature aggravate, which make the face become coarse. The top surface shows an obvious rough concave-convex shape with serration feature.

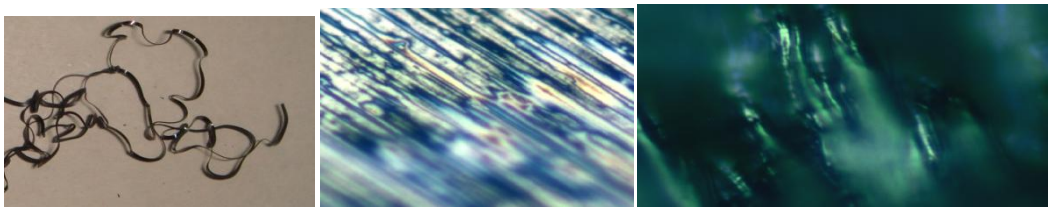

(a)Macroscopic shape (b)Undersurface(50X) (c)Top face(50X)

Figure.3. chip shape (v_c=474.925m/min, f=0.1mm/r, a_p=0.25mm)

(4)When the cutting speed, amount of feed and depth of cut are v_c=560.49m/min, f=0.083mm/r, a_p=0.25mm, respectively, the macroscopic shape of chip is showed in Fig.4 (a). It is a curly band. Compared with the chip in Fig.1 (a), the bend radius and toughness of the chip all become big. This is due to the decrease of amount of feed and thickness of the chip, its toughness corresponding increase which is helpful to remove chip. The micrographs of the chip underside and top face are illustrated in Fig.4 (b) and (c), respectively. There are trace of burn and develop tumor clipped from the rough underside. It can also be found that there is serration features from top face of chip, which shows an intense slip deformation in this cutting speed. It is because high cutting speed makes the slip velocity fast and the shearing process finished at a moment. Besides, the quantity of heat concentrates on the shear area and it is too late to spread about, then local soften adiabatic shear is formed. But because of high toughness and plasticity of high manganese steel itself, a dissociated piece not get at last.

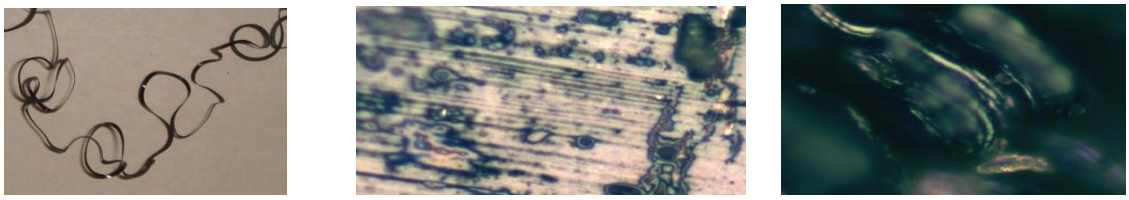

(a)Macroscopic shape (b)undersurface(50X) (c)Top face(50X)

Figure.4. Chip shape (v_c=560.49m/min, f=0.083mm/r, a_p=0.25mm)

(5)When the parameters of cutting speed and amount of feed and depth of cut are v_c=688.84m/min, f=0.067mm/r, a_p=0.25mm, respectively, the shape of chip is illustrated in Fig. 5(a). The chip appears a continuous uniform C-shape wave. This is due to a smaller amount of feed and thickness of cut and high cutting speed, which enhances the toughness of chip. The micrographs of undersurface and top face of chip are shown in Fig.5 (b) and (c), respectively. There is a trace of discontinuous cold welding clip phenomenon happened on the chip undersurface which indicates a high cutting temperature and a develop tumor formed on the rake face of the cutter when it flowing along the face. It also causes an adhesive wear of the rake face. The micrograph of chip top surface presents rugged peak valley. There are some melting pools highlighting under optic electron microscope.

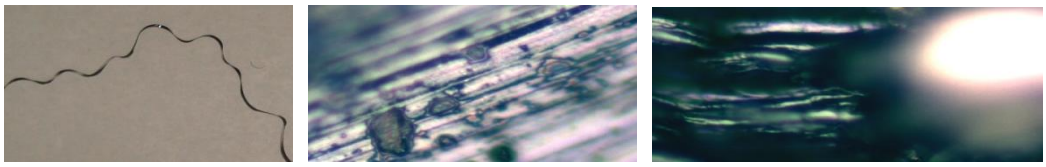

(a)Macroscopic shape (b)Undersurface(50X) (c)Top face(50X)

Figure.5. Chip shape (v_c=688.838m/min, f=0.067mm/r, a_p=0.25mm)

In conclusion, in the process of high-speed machining high manganese steel, chip presents a macroscopic continuity with the performance of plastic cutting deformation. But different shapes of chip can be found under different cutting parameters. Under the condition of testing 3(v_c=474.925m/min, f=0.1mm/r, a_p=0.25mm)and testing 4(v_c=560.49m/min, f=0.083mm/r, a_p=0.25mm), the chip shape is easier to be broken and be excluded. Serration appears on all top faces of chips in microstructure but their degree is not same. They all have the typical features of deformation similar to high-speed harden cutting, such as high temperature and local melting pool and cold welding clipping. The features prove that coherence between chip and rake face of tool appears, and develop tumor has been formed on rake face of cutter. The chip shape is due to the effect of adiabatic shear to make the shear slipping area narrow at high-speed cutting, and the heat transformed from cutting deformation work form a high-temperature concentrated heat-source because there is not enough time to transmit. The chip is then gotten with adiabatic shear. When chip flows along the rake face of tool it produces more heat with friction taken place between them, the temperature on underside rises and the friction factor increase to form coherence and develop tumor. On the other hand, the top face of chip contacted with air cools and shrinks quickly while the chip underside contacted with the rake face of cutter is not easy cold and keep high temperature, which makes the top face keep a pulling stress and undersurface keep a pressure stress. Two sides of the chip also suffer from different tensile stress because of contacting with air. The larger is the stress near to the outer side, is it the larger on the top face. So cracks are produced on top face of the chip appearing serration and pressure stress on undersurface make the chip keep continuous state in view sight.

Model of Surface Roughness

Setup of Regression Method of Roughness Model

The surface roughness value measured in cutting test is showed in table 4. To obtain the relation of roughness value with cutting parameters, we deal with the cutting parameters and roughness values according to least square method. Let's suppose the mathematic model of it as

$$y_\alpha = \beta_0 + \beta_1(x_{\alpha 1} - \overline{x}_1) + \beta_2(x_{\alpha 2} - \overline{x}_2) + \varepsilon_\alpha \tag{1}$$

Where α (equals 1, 2, …, N) is time, here N=5, y_α represents as measured value of roughness Ra, $x_{\alpha 1}$ as cutting speed, (m/min), and $x_{\alpha 2}$ as amount of feed, (mm/r), and β_0 is a constant, β_1 and β_2 are coefficients of $x_{\alpha 1}$ and $x_{\alpha 2}$, respectively, and ε_α is a random variable caused by random factors when all test points have not been on the same straight line, and y_α is also a random variable affected by ε_α.

Table 4. Cutting parameters and roughness values

Test number(N)	1	2	3	4	5
Cutting speed v_c/(m/min)	245.31	386.22	474.925	560.49	688.84
Feed f/(mm/r)	0.2	0.125	0.1	0.083	0.067
Roughness value Ra/(μm)	3.05	1.5	1.79	1.67	1.76

According to Eq. (1) , assume the regression equation required is

$$\hat{y}_\alpha = b_0 + b_1(x_1 - \overline{x}_1) + b_2(x_2 - \overline{x}_2) \tag{2}$$

Where $\hat{y}_\alpha$ a regression value, and b0, b1, b2 is are the regression coefficients of the regression equation, which of them are the estimation of parameters β_0, β_1, β_2 in Eq. (1) by least square method.

By means of a series of specific calculations, we obtain the regression values and the mean values of the parameters, respectively.

$$\begin{pmatrix} b_0 \\ b_1 \\ b_2 \end{pmatrix} = b = A^{-1}B = \begin{pmatrix} 1.9540 \\ 0.0013 \\ -5.7828 \end{pmatrix}, \quad \overline{x}_1 = 471.157, \quad \overline{x}_2 = 0.115$$

Thus the required regression equation is

$$\begin{aligned} \hat{y}_\alpha &= b_0 + b_1(x_1 - \overline{x}_1) + b_2(x_2 - \overline{x}_2) \\ &= 1.954 + 0.0013(x_1 - 471.157) - 5.7828(x_2 - 0.115) \\ &= 2.0065 + 0.0013x_1 - 5.7828x_2 \end{aligned} \tag{3}$$

Verification of the Effectiveness of the Regression Equation

To check the predict accuracy of the above model obtained, the roughness values computed with cutting parameters are compared with the measured ones. The computation results are showed in Table 5.

Table 5. Predicted values of roughness and their errors relative to experimental one

Test number (N)	1	2	3	4	5
Cutting speed v_c/(m/min)	245.31	386.22	474.925	560.49	688.84
Feed f/(mm/r)	0.2	0.125	0.1	0.083	0.067
Measured value Ra/(μm)	3.05	1.5	1.79	1.67	1.76
Computation R/a/(μm)	1.17	1.786	2.05	2.255	2.515
Relative error (%)	61.6	16	12.7	25.9	30

The results of calculation and measured value compared in table 5 are uniform among 12.7~30 except for test 1, and the distribution of calculated value is relative balance without abnormity. The unusual value measured in test 1 may be inaccurate in measurement to cause a big error. Totally, the results of the prediction and measurement are rather near. Therefore, the roughness model can be used to predict the surface quality or choose cutting parameters in high-speed cutting.

Tool Wear

Tool abrasion loss is measured by means of tool microscope. The results of rake face and back face wear measured are showed in table 6. The numerical values in parenthesis are height of develop tumor. For convenient analysis and comparison, it is illustrated in histogram in Fig.6.

Table 6. Wear loss of rake face and rear face

Test number (N)	1	2	3	4	5
Cutting speed v_c/(m/min)	245.31	386.22	474.925	560.49	688.84
Feed f/(mm/r)	0.2	0.125	0.1	0.083	0.067
Rake face wear KT/(mm)	0.27	0.78(0.225)	1.45(0.16)	0.75(0.09)	0.8(0.24)
Back face wear VB/(mm)	0.165	0.342	0.45	0.66	0.08

It is observed that the wear loss of the rake face in test 3 is small while it is the smallest in test 3. The wear loss of the flank face in test 5 is the smallest while it is the biggest in test 4. Comprehensive analysis, the wear loss of tool rake face and back face in test 1 is small without forming develop tumor. The reason of it is that the cutting speed and cutting temperature are relative lower in test 1, the tool wear is not caused by adhension. With cutting speed rise, the cutting temperature sharply goes up and friction coefficient enlarges, which makes adhension worsen. So the adhesive wear plays a leading role in a serious wear of rake face. When the cutting speed surpasses the critical point, the cutting temperature and the cohesive degree falls, which leads to a low abrasion of the tool rake face. The above statements indicates that the Salomon' theory on

high-speed cutting is right. The wear loss of flank face rises with increase of cutting-speed, but it becomes smaller after test 4. The truth can be used to improve a tool life when cutting speed is increased to a certain value.

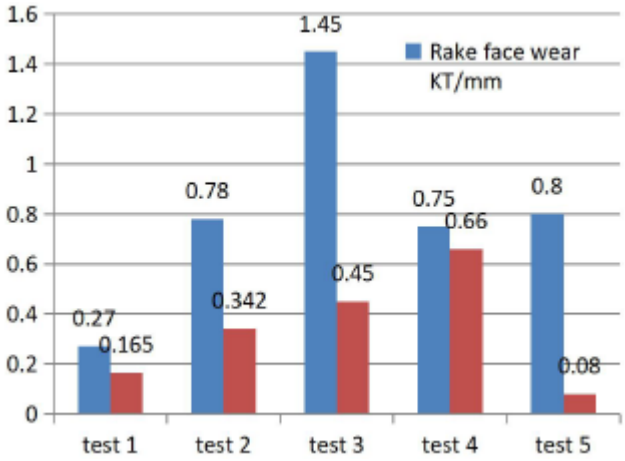

Figure.6. Histogram of tool wear

Conclusions

(1)The chip presents a continuous shape in macroscopic view and a serration on top surface in microscopic view when cutting high manganese steel at high-speed cutting. High cutting temperature produces an adhesive phenomenon between the undersurface of chip and rake face of tool, so the tool wear is mainly adhesive wear.

(2)The metal ceramic tool can be used to cut high manganese steel at high-speed cutting, the machined-surface quality can basic satisfy the demand of finish machining. Processing quality would be further improved when optimizing technological parameters with test results or improving cutting conditions.

(3)The roughness model obtained can be used to predict processing quality in a certain precision range according to the cutting parameters. Conversely, in HSC technology, the prediction model can also be used to decide cutting parameters by a simple calculation according to a demanded roughness.

(4)The reason of macroscopic succession and microscopic serration in a chip deformation of high manganese steel are in two aspects. First, because the toughness and plasticity of the material itself is strong and is not easy to break off. Second, high stress gradient and temperature gradient exist between top face and undersurface of a chip in high-speed cutting process. Especially, it results from the tensile stress on top face and the pressure stress on undersurface of a chip.

Acknowledgements

The authors are grateful to the Natural Science Foundation of Gan-Su Province, China (Grant no. 145RJZA134) and the Science Technology Program of Lan-Zhou City, Gan-Su Province, China (Grant no.2015-3-99) and Lan-Zhou City University President Science and Research Innovation Foundation (Grant no.LZCU-XZ2014-01) for financial support in this investigation.

References

1. Hu Y.K., Li S.J.. Research on cutting technology of machining high manganese steel [J].Mechanic Engineering and automation, 2011.11, 164(1): 176-177, 180.

2. Xu L., Teng T., Yang L. et al. Research on constitutive equation and simulation test of ZGMn13 High manganese steel [J]. Manufacturing technology and machine tool, 2011(10): 62-65.

3. Xu Y.D., Liu N., Li Z.D.. Research on the wear performance of metal ceramic tool cutting difficult-to-machining materials [J]. Tool engineering, 2002.8, 36(10): 8-10.

4. Liu L.L.. Research on the matching of the ceramic tool and difficult-to-machining materials [J]. Mechanic Engineering materials. 2004.8, 28(8):1-3, 41.

5. Liu Z.Q., Ai X. Research on the morphology of wear surface of high-speed cutting tool. Tribulogy Journal, 2002,22(6): 468-471.

6. Ai X., Liu Z.Q., Huang C.Z. et al. Composite technology of high-speed cutting [J]. Air aeronautic manufacturing technology. 20029(3): 20-23.